JOURNAL OF MATERIALS SCIENCE **39** (2004) 6057– 6066

Carbothermal reduction synthesis of nanocrystalline zirconium carbide and hafnium carbide powders using solution-derived precursors

MICHAEL D. SACKS, CHANG-AN WANG*, ZHAOHUI YANG, ANUBHAV JAIN
School of Materials Science and Engineering, Georgia Institute of Technology, Atlanta, GA 30332-0245, USA
E-mail: michael.sacks@mse.gatech.edu

Zirconium carbide (ZrC) and hafnium carbide (HfC) powders were produced by the carbothermal reduction reaction of carbon and the corresponding metal oxide (ZrO_2 and HfO_2, respectively). Solution-based processing was used to achieve a fine-scale (i.e., nanometer-level) mixing of the reactants. The reactions were substantially completed at relatively low temperatures ($<1500^{\circ}C$) and the resulting products had small average crystallite sizes (~50–130 nm). However, these products contained some dissolved oxygen in the metal carbide lattice and higher temperatures were required to complete the carbothermal reduction reactions. Dry-pressed compacts prepared using ZrC-based powders with ~100 nm crystallite size could be pressurelessly sintered to ~99% relative density at 1950°C. © *2004 Kluwer Academic Publishers*

1. Introduction

Zirconium carbide (ZrC) and hafnium carbide (HfC) are of interest for ultrahigh temperature applications because of their high melting points (~3550 and ~3900°C, respectively), solid-state phase stability, and good thermomechanical and thermochemical properties [1–5]. Other desirable properties of ZrC and HfC include high hardness and wear resistance, high emissivity, and high current capacity at elevated temperatures. Hence, these carbides are promising materials for cutting tools, thermophotovoltaic radiators, and field emitter tips and arrays [1, 2, 6, 7]. In addition, ZrC is useful as a nuclear reactor core material because of its low neutron cross-section [8].

ZrC and HfC are usually synthesized by reacting powder mixtures of carbon and the corresponding metal (Hf, Zr), metal hydride (ZrH_2, HfH_2), or metal oxide (ZrO_2, HfO_2) [1, 2, 5, 6, 9–13]. In most cases, high temperatures are required for the carbide-forming reactions because the powders are mixed together on a relatively coarse scale (e.g., micrometer-scale). This also leads to metal carbide products with relatively large particle sizes. Hence, hot pressing is usually necessary to produce bulk objects with high relative densities.

Recent studies have shown that ZrC and HfC can be synthesized at lower temperatures by using precursors that have been prepared by solution-based processing methods [14–18]. Sham *et al*. synthesized ZrC powders using mixed solutions of zirconium *n*-propoxide (as a zirconia source) and either ethylene glycol or 1,4 benzenediol (as a carbon source) [14]. Preiss *et al*. used chelated derivatives of zirconium *n*-propoxide and various soluble carbon-bearing compounds (including those used by Sham *et al*.) to form ZrC fibers, films, and powders [15]. Hasegawa *et al*. used mixtures of zirconium 2,4,-pentanedionate and phenolic resins to produce ZrC fibers with diameter ≥ 60 μm [16]. Hu *et al*. used the same mixtures to produce nanocrystalline ZrC powders and fibers with ~20 μm diameter [17]. Kurokawa *et al*. produced large-diameter (≥ 50 μm) ZrC and HfC fibers by using solutions containing cellulose acetate and metal alkoxides (zirconium *n*-butoxide and hafnium isopropoxide) as the precursors for the carbon and metal oxides, respectively [18]. The aforementioned studies all showed (via X-ray diffraction analyses) that ZrC or HfC phases can be formed at relatively low temperatures compared to conventional methods. However, very little information on the densification behavior of these materials was presented and it was not reported if bulk samples could be fabricated by pressureless sintering.

In the present study, ZrC- and HfC-based precursors with a range of carbon/metal oxide ratios were prepared from chelated derivatives of metal alkoxides by varying the hydrolysis conditions and by adding soluble secondary "carbon sources" (i.e., glycerol and phenolic resin) during solution-based synthesis. The solution-derived precursors were given heat treatments

Present address: Department of Materials Science and Engineering, Tsinghua University, Beijing 100084, People's Republic of China.

(pyrolysis and carbothermal reduction) to produce nanocrystalline ZrC and HfC powders. Pressureless sintering of the ZrC powder was investigated.

2. Experimental

The processing steps used to produce ZrC and HfC are initially described below in broader terms in order to provide the rationale for the synthesis methodology. This is followed by the specific experimental details used in the synthesis and characterization of each individual metal carbide.

The synthesis approach is illustrated via the flow chart in Fig. 1. A metal alkoxide, either self-synthesized or obtained from a commerical vendor, was used as an alcohol-soluble precursor for the formation of the metal oxide reactant needed for the carbothermal reduction reaction. The metal alkoxide is refluxed with 2,4 pentanedione (also known as acetylacetone and often referred to as "acacH") in order to partially or fully convert the metal alkoxy groups to a chelated metal diketonate structure (i.e., a metal pentanedionate, or "metal acac," in this case). (The extent of replacement depends on factors such as the reflux time/temperature schedule, "acacH"/metal alkoxide ratio, and solvent concentration.) The primary reason for carrying out the replacement reaction is to produce a soluble metal-organic precursor that allows for greater control over the hydrolysis and condensation reactions that are carried out in a subsequent processing step. In general, metal alkoxides undergo more rapid hydrolysis/condensation reactions than the corresponding metal diketonates and this may result in uncontrolled precipitation of relatively large precursor particles. The replacement reaction also allows for more control over the carbon/metal oxide ratio in the pyrolyzed powders that are subsequently produced (and used for the carbothermal reduction reactions). For example, pyrolyzed materials with higher carbon contents can be obtained by using precursors with a higher degree of replacement of the alkoxide groups. The flow chart in Fig. 1 also shows that another method for increasing the carbon/metal oxide ratio in the pyrolyzed product is to combine the metal-organic precursor with a soluble carbon-bearing source in a mutually compatible solvent. This can be done prior to or after the "acacH" refluxing step.

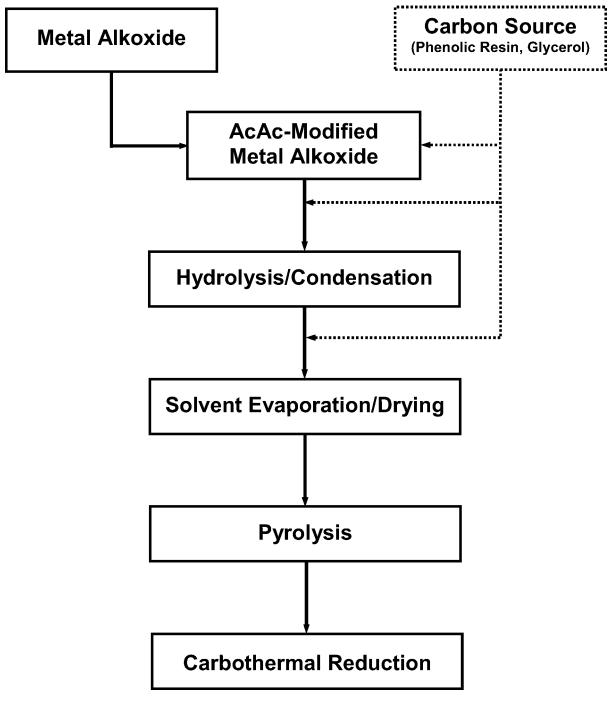

Figure 1 Flow chart for synthesis of metal carbide from solution-based precursors.

The next solution processing step is to hydrolyze the metal-organic precursor through the addition of water. Hydrolysis is required to initiate condensation reactions which, in turn, lead to the build-up of sol species with three-dimensional structure. (The latter development is important in order to obtain a reasonable ceramic yield upon subsequent pyrolytic decomposition.) The extent of the hydrolysis/ condensation reactions depends on the water concentration and solution pH. The latter variables can be used to alter the size and chemical composition (i.e., metal/oxygen/carbon content) of the sol species (and the powder product that is subsequently obtained).

After the hydrolysis/condensation step, the solvent is evaporated and a dried powder product is obtained. This is followed by sequential heat treatments to (i) pyrolytically decompose the dried product and thereby form a nano-scale carbon/metal oxide mixture and (ii) form the metal carbide by carbothermal reduction reactions.

2.1. Zirconium carbide

The starting Zr-containing material was a zirconium *n*-propoxide/*n*-propanol solution (i.e., 70 wt% $Zr(OC_3H_7)_4$ in *n*-propanol, Alfa Aesar, Ward Hill, MA). The zirconium *n*-propoxide was mixed with "acacH" (i.e., 2,4-pentanedione, Alfa Aesar, Ward Hill, MA) using molar ratios in the range of 0.25–0.33. (Ethanol was used as a mutual diluent.) The resulting solutions were refluxed at temperatures in the range of 130–195°C for 2 h. After refluxing, much of the solvent was evaporated (to remove residual propanol and residual "acacH") and then ethanol was added back to the sol (ethanol/Zr molar ratios in the range of ~100–200). The refluxed Zr-containing precursors were partially hydrolyzed (at 50°C for 2 h) using acidic conditions (HNO_3/Zr molar ratios in the range of 0.04–0.27) and an H_2O/Zr molar ratio of 24. Glycerol ($C_3H_8O_3$, Fisher Scientific, Fair Lawn, NJ) or phenol-formaldehyde resin ("novolac" type, Georgia Pacific, Atlanta, GA) were added to some solutions to increase the C/Zr ratio in the powders used for carbothermal reduction. Glycerol additions were made directly to refluxed solutions (i.e., prior to hydrolysis) using glycerol/Zr molar ratios in the range of 0.17–0.63. In contrast, phenolic resin was added to hydrolyzed solutions as an ethanol-based solution at a 1:1 molar ratio of C:Zr. Hydrolyzed solutions were initially concentrated by rotary evaporation and then dried to powders at 120°C (2 h).

The dried powders were subsequently pyrolyzed at temperatures in the range of 800–1100°C (1–2 h) in a flowing argon atmosphere to produce carbon/zirconia

mixtures. The C/Zr ratios in some of the pyrolyzed (1100°C, 1 h) samples were determined from weight losses that occurred upon further heat treatment (1100°C, 1 h) in air (i.e., in order to remove carbon by oxidative combustion). Sample weight losses during argon pyrolysis and oxidative combustion were also monitored in-situ using thermal gravimetric analysis, TGA (Model STA 409, Netzsch, Exton, PA). Pyrolyzed powders were subsequently heat treated at temperatures in the range of 1200–1800°C (2 h) in flowing argon. Selected heat-treated samples were characterized for weight loss, phase development, chemical composition, and crystallite size.

X-ray diffraction, XRD (Model PW1800, Philips Analytical, Netherlands), was used to determine the phases present and the ZrC lattice parameters in selected powder samples. In addition, ZrC and ZrO_2 crystallite sizes were calculated from the broadening of the XRD peaks using the Scherrer Equation [19]. Selected pyrolyzed and carbothermally-reduced powders were analyzed for carbon and/or oxygen content based on analysis of the CO_2 evolution during oxidative combustion (Sherry Laboratories, Muncie, IN; LECO Corp., St. Joseph, MI).

The sintering behavior was evaluated using a ZrC-based powder prepared by carbothermal reduction at 1475°C. The powder was milled for 10 min to break up aggregates using a Spex mill (Model 8000, Spex Certiprep, Metuchen, NJ). The milled powder was mixed with approximately 10 vol% organic binder (polyvinyl alcohol/polyethylene glycol mixture) and dry pressed at ~250 MPa using a steel die with a cylindrical cavity. The binder was removed by heat treatment at 1150°C (1 h in argon). All samples were initially "pre-sintered" at 1600°C (2 h in argon) and then subsequently sintered at temperatures in the range of 1725–1950°C (2 h in argon). The bulk densities of the samples were determined based on the weight and geometric dimensions of the cylinder-shaped samples. In addition, the bulk density and open porosity were determined for some samples using the Archimedes displacement method with distilled water as the suspending liquid. Relative (percentage) densities were calculated using a solid ("true") density value that was determined from the XRD lattice parameter measurement.

2.2. Hafnium carbide

The starting material for HfC synthesis was hafnium tetra-chloride ($HfCl_4$, Alfa AESAR, Ward Hill, MA). This was used to synthesize hafnium tetra-isopropoxide, $Hf(OC_3H_7)_4$, following procedures in the literature [20, 21]. The hafnium isopropoxide was mixed with a large excess of "acacH" (i.e., Hf propoxide/"acacH" molar ratios in the range of 0.020–0.033) with reagent-grade (Fisher Scientific, Suwanee, GA) propanol/benzene solutions as a mutual diluent. Mixed solutions were refluxed at temperatures in the range of 145–155°C for 4 h. After refluxing, most of the solvent was evaporated (to remove residual "acacH," propanol, and benzene) and then ethanol was added back to the sols (ethanol/Hf molar ratios in the range of 400–500). The Hf-containing precursors were then hydrolyzed at 45°C (1 h) under acid conditions using an H_2O/Hf molar ratio of 16 and HNO_3/Hf molar ratios in the range of 0.18–1.54). It should be noted that a secondary soluble carbon source was *not* added to any of metal-organic solutions, either prior to or after the hydrolysis/condensation step. Solutions were then given the various heat treatment steps (i.e., solvent evaporation/drying, pyrolysis, and carbothermal reduction) in the same manner as described for the ZrC synthesis.

The synthesized products were characterized using the same methods described earlier. In addition, some Hf-based solutions and powders were characterized by Fourier transform infrared spectroscopy, FTIR (Model Nexus 870, Nicolet Instrument Corp., Madison WI). An as-synthesized hafnium propoxide solution was concentrated (~84 wt% propoxide solution) and subsequently loaded (under inert atmosphere) into a KBr liquid cell for FTIR analysis. A sample refluxed with "acacH" was concentrated (~4 wt% solution) and subsequently deposited onto a porous KBr powder compact. Vacuum was then applied to the solution-infiltrated compact to remove most of the solvent prior to FTIR analysis. An Hf-based powder produced after the hydrolysis, concentration, and drying steps was mixed with KBr powder and pressed into a compact for the FTIR analysis. (The two samples prepared with KBr powder had exposure to the ambient air atmosphere, so some adsorbed moisture was present in the compacts.)

3. Results and discussion

3.1. Zirconium carbide

An idealized reaction to produce stoichiometric ZrC by carbothermal reduction (CTR) involves reacting carbon and zirconia in a 3:1 molar ratio:

$$3C_{(s)} + ZrO_{2(s)} = ZrC_{(s)} + 2CO_{(g)} \qquad (1)$$

In this study, powders with different C/ZrO_2 ratios were prepared by varying the solution synthesis conditions. For example, Fig. 2 shows that C/Zr molar ratios in pyrolyzed samples (1100°C, 1 h) were varied in the range of ~1.6 to ~2.4 by changing the HNO_3/Zr molar ratio (from 0.42 to 0.12, respectively) during solution synthesis. (In these experiments, the Zr propoxide/"acacH" molar ratio used in the refluxing step (at 195°C) was 0.33 and the H_2O/Zr ratio used in the hydrolysis/condensation step was 24.) Samples with higher C/Zr molar ratios were produced using solutions with glycerol or phenolic resin additions. Fig. 3 shows that samples with C/Zr molar ratios in the range of ~2.4 to ~3.5 were prepared by using glycerol/Zr molar ratios in the range of 0 to 0.63, respectively, during solution synthesis. (The HNO_3/Zr molar ratio was 0.27 and the "acacH" and water concentrations were the same as used for the samples in Fig. 2.) Fig. 4 shows a typical TGA plot of residual weight vs. temperature for a solution-derived powder (dried at 120°C, 2 h) which was heated (in argon) to 1100°C and held at temperature for 1 h. (The sample was prepared using molar ratios of 0.25 for Zr propoxide/"acacH," 0.04 for HNO_3/Zr, and 24 for H_2O/Zr. Phenolic resin was added at a C/Zr

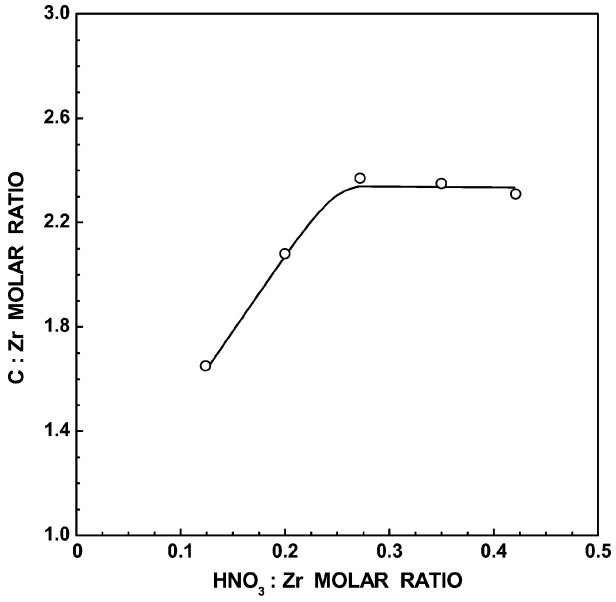

Figure 2 Plot of C/Zr molar ratio in pyrolyzed (1100°C, 1 h) samples that were prepared using varying HNO_3/Zr molar ratios during solution synthesis.

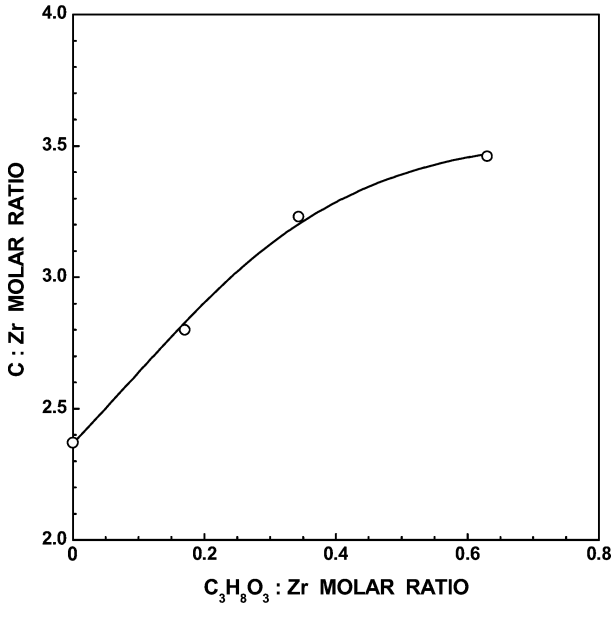

Figure 3 Plot of C/Zr molar ratio in pyrolyzed (1100°C, 1 h) samples that were prepared using varying glycerol/Zr molar ratios during solution synthesis.

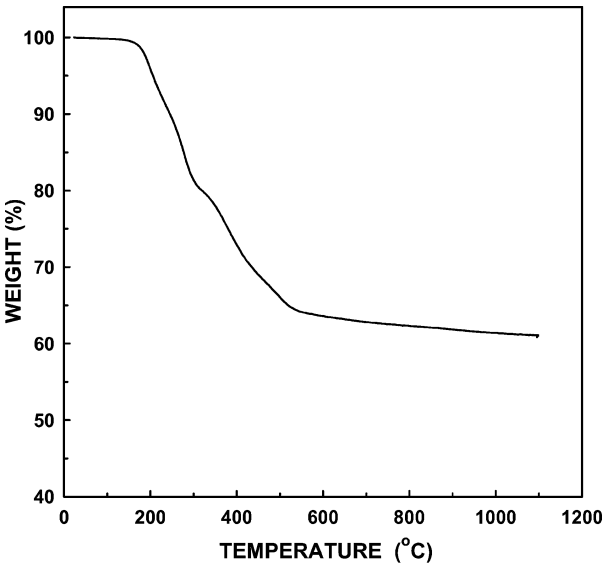

Figure 4 TGA plot of weight loss vs. temperature for an as-dried (120°C) precursor prepared from a (zirconium *n*-propoxide/phenolic resin)-based sol.

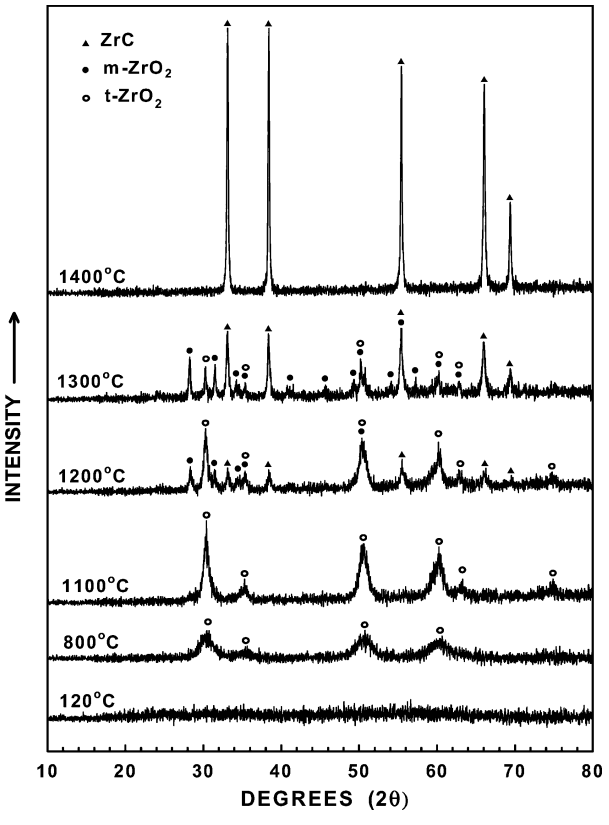

Figure 5 X-ray diffraction patterns for as-dried (120°C) and heat treated (800–1400°C) samples prepared from a (zirconium *n*-propoxide/phenolic resin)-based sol.

molar ratio of 1.0.) Fig. 4 shows that pyrolytic decomposition of the mixed precursor was mostly completed by ~550°C, although small weight losses were observed throughout the rest of the heat treatment. (There was also a small weight loss of ~0.4% observed during the 1 h hold at 1100°C.)

Fig. 5 shows X-ray diffraction (XRD) results for as-dried (120°C) and heat treated samples (2 h at 800–1400°C in argon) prepared from the same powder that was used for the TGA experiment in Fig. 4. The as-dried powder was amorphous. The XRD pattern for a sample pyrolyzed at 800°C (2 h) shows weak and broad diffraction peaks that are due to tetragonal zirconia (t-ZrO_2). The carbon present in the sample remained amorphous. The only significant change in the XRD pattern for a sample heat treated at 1100°C (2 h) is that the t-ZrO_2 peaks increased in intensity.

The initial formation of ZrC was observed in the sample that was heat treated at 1200°C (Fig. 5). The XRD pattern for this sample also shows that some t-ZrO_2 had transformed to monoclinic ZrO_2 (m-ZrO_2). ZrC became the predominant phase after heat treatment at 1300°C, although a substantial amount of m-ZrO_2 and t-ZrO_2 were still present. ZrC was the only crystalline phase observed in the samples heat treated at 1400°C

TABLE I Chemical analysis and lattice parameter values of ZrC powders

Processing temperature (°C)	Carbon concentration (wt%)	Oxygen concentration (wt%)	Lattice parameter (nm)
1025	23.3	n.d.	n.d.
1300	n.d.	n.d.	0.4694
1400	n.d.	n.d.	0.4691
1475	13.4	3.3	0.4691
1800	11.3	0.1	0.4696

(Fig. 5) and at higher temperatures (not shown in Fig. 5). However, characterization results described below (i.e., measurements of weight loss, carbon and oxygen contents, and lattice parameter) show that the 1400°C sample was *not* phase-pure stoichiometric ZrC. Instead, the sample consisted of "zirconium oxycarbide" (i.e., ZrC with some oxygen dissolved in the lattice) and some residual amorphous carbon.

Table I shows the carbon and oxygen contents for samples prepared from the same powder used in the TGA and XRD experiments (Figs 4 and 5). A sample pyrolyzed at 1025°C (2 h) had a carbon content of 23.3 wt%. (This is equivalent to a C/Zr molar ratio of 3.1, i.e. assuming that the pyrolyzed material contained only ZrO_2 and C.) Table I also shows that subsequent heat treatment at 1475°C (2 h) produced a sample with 13.4 wt% carbon. This carbon content is greater than the value of 11.6 wt% that would be expected if the sample was phase-pure stoichiometric ZrC. Hence, it is apparent that the sample retained some free carbon (XRD-amorphous) after the heat treatment. Furthermore, the sample also contained 3.3 wt% oxygen. Since ZrO_2 is not observed in XRD patterns for samples heat treated at or above 1400°C, it is evident that the oxygen present in the sample was dissolved in the zirconium carbide lattice.

Table I also shows that further heat treatment at 1800°C (2 h) produced a sample with carbon concentration (11.3 wt%) equivalent to that of stoichiometric ZrC (i.e., within experimental error of the measurement). In addition, the oxygen content was reduced to a very low level (0.1 wt%). The decrease in carbon and oxygen contents for the 1800°C sample is consistent with weight loss behavior that was observed (see Fig. 6) when 800°C-pyrolyzed powder was heat treated at temperatures in the range of 900–1800°C for 2 h. Fig. 6 shows that there was still a significant weight loss upon heat treatment above 1400°C, even though samples heat treated at (or above) this temperature showed no residual ZrO_2 in the XRD patterns (Fig. 5). In combination, the weight loss (Fig. 6) and the decrease in carbon and oxygen contents (Table I) upon heat treatment to 1800°C can be explained by a carbothermal reduction reaction in which the reactants were zirconium oxycarbide and free carbon:

$$ZrO_yC_{(1+y-x)(s)} + xC_{(s)} = ZrC_{(s)} + yCO_{(g)} \qquad (2)$$

The present study is consistent with previous studies which have shown that there is considerable solid

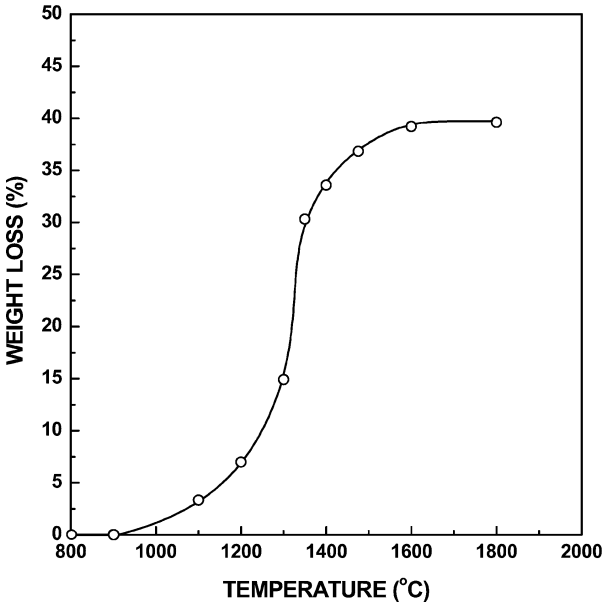

Figure 6 Plot of weight loss vs. temperature for an 800°C-pyrolyzed sample prepared from a (zirconium *n*-propoxide/phenolic resin)-based sol.

solubility of ZrO_2 in ZrC [10, 22–24]. The ZrC (face-centered cubic) lattice parameter decreases with increasing amount of dissolved oxygen [10,22–24]. Table I shows the ZrC lattice parameters for samples prepared in this study. The lattice parameter was 0.4694 nm for the 1300°C sample. The value decreased to 0.4691 nm for the ZrC in the 1400 and 1475°C samples. This indicates that either some zirconia dissolved in the ZrC lattice as the heat treatment temperature was increased (from 1300 to 1475°C) or that direct formation of an oxycarbide composition (instead of stoichiometric ZrC) was more favorable at the higher reaction temperatures (i.e., at 1400 and 1475°C). With further heat treatment at 1800°C, the ZrC lattice parameter increased to 0.4696 nm. This result is again consistent with the reaction shown in Equation 2 in that the lattice parameter increased to a value that is expected for near-stoichiometric ZrC [22–24].

Fig. 7 shows the average crystallite sizes (determined by XRD measurements on the same samples shown in Fig. 5) for each phase (ZrC, *t*-ZrO_2, and *m*-ZrO_2) as a function of heat treatment temperature. The *t*-ZrO_2 crystallites remain relatively small (<20 nm) in the pyrolyzed samples (800–1100°C). Rapid crystallite growth begins with the onset of the carbothermal reduction reaction above 1100°C. The crystallite sizes for both the *t*-ZrO_2 and *m*-ZrO_2 phases increased from ~30–45 nm at 1200°C to ~110–130 nm at 1350°C. The ZrC crystallites also increased from ~40 nm in the early stages of the reaction (1200°C sample) to ~120 nm in the 1400°C sample (which contained no ZrO_2 second phase). The close correspondence in crystallite size growth for the ZrC and two ZrO_2 phases is consistent with certain aspects of the reaction mechanism suggested by Maitre *et al.* [24] in a carbothermal reduction study carried out using mixtures of ZrO_2 and C powders. In particular, they proposed that the transformation proceeded by the "contracting volume"

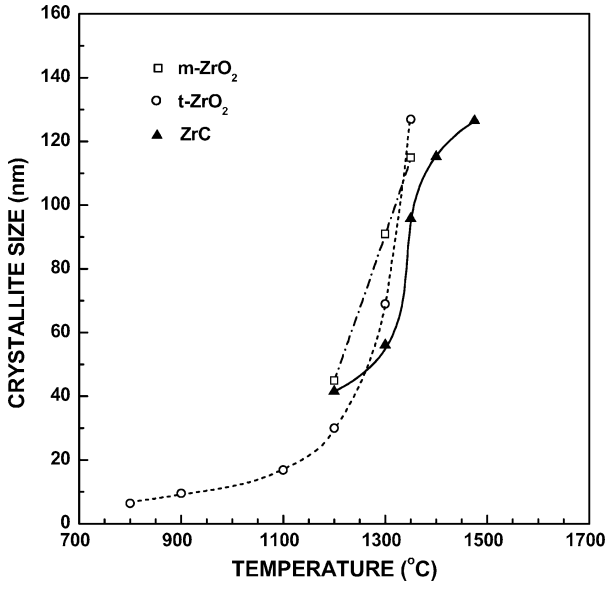

Figure 7 Plots of the *t*-ZrO_2, *m*-ZrO_2, and ZrC crystallite sizes (determined from XRD line broadening measurements) vs. heat treatment temperature.

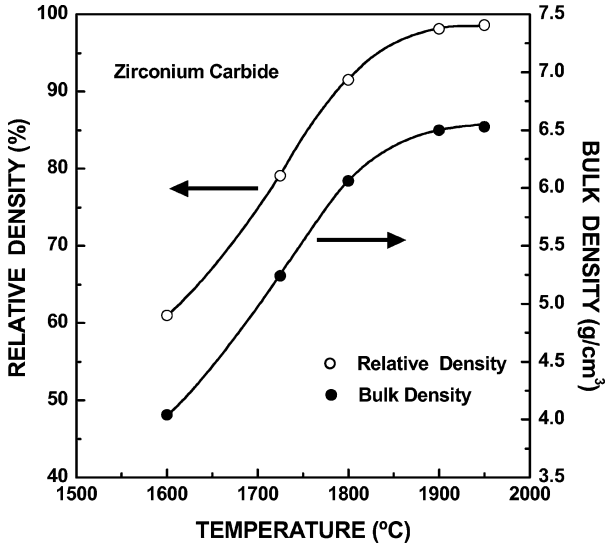

Figure 8 Plots of relative density and bulk density vs. sintering temperature for dry-pressed ZrC powder compacts.

mechanism in which growth of ZrO_xC_y proceeds from the surface to the interior of the ZrO_2 particles.

The densification behavior was investigated using a powder which had a slightly carbon-deficient composition (relative to stoichiometric ZrC) after sintering. The powder was prepared using molar ratios of 0.33 for Zr propoxide/"acacH," 0.27 for HNO_3/Zr, and 24 for H_2O/Zr. The "acacH" refluxing temperature was 195°C. Phenolic resin was added at a C/Zr molar ratio of 1.0. The heat treatment conditions for pyrolysis and carbothermal reduction were 800°C (2 h) and 1475°C (2 h), respectively. The reacted powder was milled for 10 min prior to dry pressing. The XRD pattern for this powder showed ZrC as the only crystalline phase. The crystallite size determined by XRD line broadening measurements was ~100 nm. The powder surface area was 17 m^2/g. (This surface area is equivalent to a particle size of 57 nm if the particles were non-contacting, non-porous, monosized spheres with true solid density of 6.6 g/cm^3.) Dry-pressed powder compacts had a relative "green" density of ~44% after pyrolysis of the organic binder at 1150°C (2 h). (The powder density used for the relative density calculation was 6.6 g/cm^3.)

Fig. 8 shows a plot of the sample bulk density vs. sintering temperature. The bulk densities reported in this figure were calculated from the sample weight and geometric dimensions. The bulk density and open porosity were also determined by the Archimedes displacement method for the samples sintered at 1900 and 1950°C. The bulk density measurements for the two methods gave similar values; the values for the geometric vs. Archimedes measurements were 6.50 vs. 6.53 g/cm^3, respectively, for the 1900°C samples and 6.53 vs. 6.54 g/cm^3, respectively, for the 1950°C samples. The 1900 and 1950°C samples both showed zero open porosity from the Archimedes measurement method.

Fig. 8 also shows a plot of the relative density vs. sintering temperature for the samples. The relative densities were ~92, ~98 and ~99% for the samples sintered at 1800, 1900, and 1950°C, respectively. The relative densities for all the sintered (1600–1950°C) samples were calculated by assuming that the solid true density was 6.62 g/cm^3. The latter value was based on using the lattice parameter measured on a powder sample which had been heat treated at 1900°C (2 h) and by assuming that the sintered samples were 100% stoichiometric ZrC. In fact, samples sintered at the lower temperatures probably still had some dissolved oxygen in the ZrC lattice. (Some free carbon may have been present also.) In addition, the samples sintered at the higher temperatures were somewhat deficient in carbon relative to stoichiometric ZrC. The carbon contents measured on powder samples heat treated at 1800°C (2 h) and 1900°C (2 h) were 11.0 and 10.8 wt%, respectively. Hence, the solid true densities for the samples probably varied with sintering temperature (from 1600 to 1950°C). Nevertheless, the values are not expected to be significantly different from the assumed value of 6.62 g/cm^3.

The maximum sintered densities obtained in this study were equal to or higher than the values reported in previous studies of ZrC sintering. In addition, the sintering temperatures (1900–1950°C) were lower. Nezhevenko *et al*., Bulychev *et al*., and Lanin *et al*. reported pressureless sintering of ZrC to maximum relative densities of 97–98% using temperatures in the range of 2400–2600°C [25–27]. Barnier *et al*. [28] also reported maximum relative densities of ~97 and ~98% by hot pressing at 2000°C (2 h) and 2300°C (1 h), respectively, with an applied pressure of 40 MPa.

3.2. Hafnium carbide

Fig. 9 shows FTIR spectra for (a) concentrated (~84 wt%) hafnium propoxide solution, (b) dried sample prepared after refluxing the hafnium propoxide solution with excess "acacH," and (c) dried powder prepared after hydrolysis of the "acacH"-refluxed solution. The spectrum for the hafnium propoxide is in good agreement with results reported by Lynch *et al.*

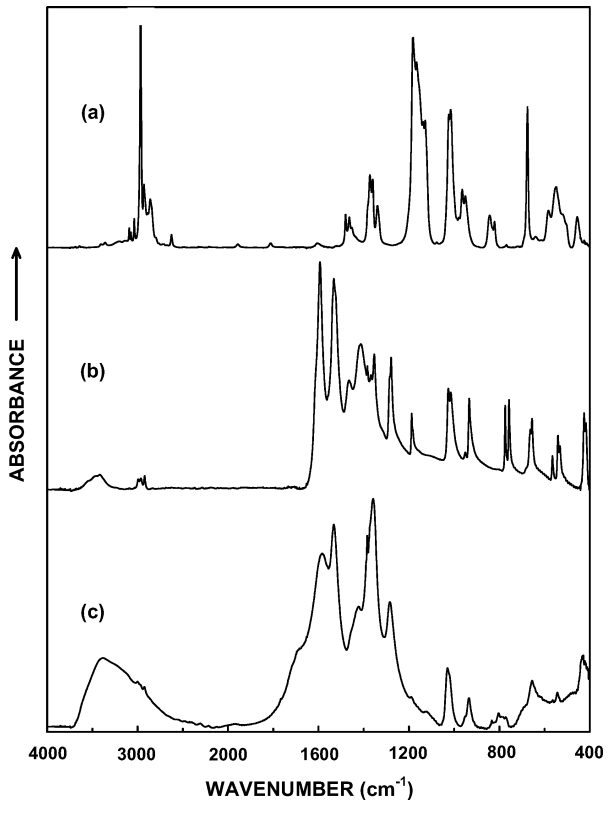

Figure 9 FTIR spectra for (a) concentrated hafnium propoxide solution, (b) dried sample prepared after refluxing the hafnium propoxide solution with acetylacetone, and (c) dried powder prepared after hydrolysis of the acacH-refluxed solution.

[29] (The latter researchers produced hafnium propoxide by the same method used in the present study, i.e., by reacting $HfCl_4$ with isopropanol.) Fig. 9a contains some additional peaks (i.e., besides those associated with hafnium propoxide) due to the solvent components in the concentrated solution (i.e., benzene and isopropanol). Fig. 9b shows the spectrum for a solution which was prepared by refluxing the hafnium propoxide solution at 155°C (4 h) with a large excess of "acacH" (i.e., molar ratio of 1:50). The propoxide was converted almost completely to hafnium 2,4 pentanedionate (i.e., "hafnium acac"). This is indicated by the close agreement of the spectral results shown in Fig. 9b with results reported by previous researchers [30, 31] and by measurements (not shown in Fig. 9) that were carried out using a commercial source of "hafnium acac" (Strem Chemicals, Newburyport, MA).

As noted earlier, metal diketonates are usually more resistant to hydrolysis compared to the corresponding metal alkoxide. This provides an advantage in subsequent processing because it allows for better control over the C/Hf ratio that is subsequently obtained after the high temperature heat treatments. Fig. 9c shows the FTIR spectrum for the powder produced after hydrolysis, concentration, and drying of the "hafnium acac" solution. (The solution was prepared using molar ratios of $H_2O/Hf = 16$ and $HNO_3/Hf = 1.4$, respectively.) Hydrolysis of the "hafnium acac" precursor is indicated by the large, broad peak for the OH stretching vibration over the range of ~2700–3700 cm^{-1}. It is evident, however, that an extensive Hf-chelate structure is still present in the as-dried powder. For example, the strong symmetric and asymmetric stretching vibrations (at ~1595 and ~1530 cm^{-1}, respectively) from C═O and C═C bonds in the chelate ring are still the most intense peaks in the spectra. Fig. 9c also shows peak broadening has occurred in the hydrolyzed sample (e.g., in the ranges ~400–800 cm^{-1} and ~1200–1800 cm^{-1}) which presumably reflects the development of a more complex and disordered structure (i.e., compared to the "Hf acac"). Hydrolysis (and subsequent condensation) reactions result in partial replacement of Hf─O─C bonds (from the "Hf acac" structure) with Hf─OH bonds and Hf─O─Hf bonds. (The substantially amorphous character of this material was confirmed by XRD analysis on a similar dried powder.)

It was possible to produce heat-treated powders (pyrolyzed and carbothermally-reduced) with a wide range of C/Hf ratios by using the fully chelated "Hf acac" compound as the starting material for the hydrolysis/condensation. The composition was varied by changing the acid and/or water concentrations used in the hydrolysis/condensation step. For example, Fig. 10 shows the effect of acid concentration (i.e., HNO_3/Hf molar ratio) on the C/Hf molar ratio in pyrolyzed samples. (For these samples the Hf propoxide/"acacH" molar ratio used for refluxing (at 155°C) was 0.02 and the H_2O/Hf ratio used for hydrolysis/condensation was 16.) Fig. 10 shows that pyrolyzed powders can be produced with a C/HfO_2 molar ratio of 3, i.e., the composition needed to produce stoichiometric HfC by carbothermal reduction. Note that this ratio was obtained without using a secondary source of soluble carbon (i.e., in contrast to the method used to produce the near-stoichiometric ZrC). Hence, near-stoichiometric HfC can be produced by using a "single-source" solution-based precursor.

Fig. 11 shows TGA results for an as-dried (120°C) precursor which was heated (in flowing argon) to 1100°C and held at temperature for 1 h. (The sample was prepared using molar ratios of 0.02 for Hf

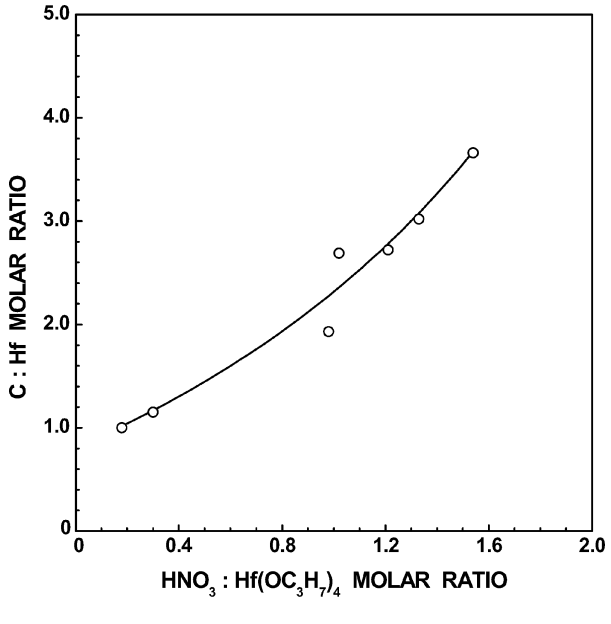

Figure 10 Plot of C/Hf molar ratio in pyrolyzed samples that were prepared using varying HNO_3/Hf molar ratios during solution synthesis.

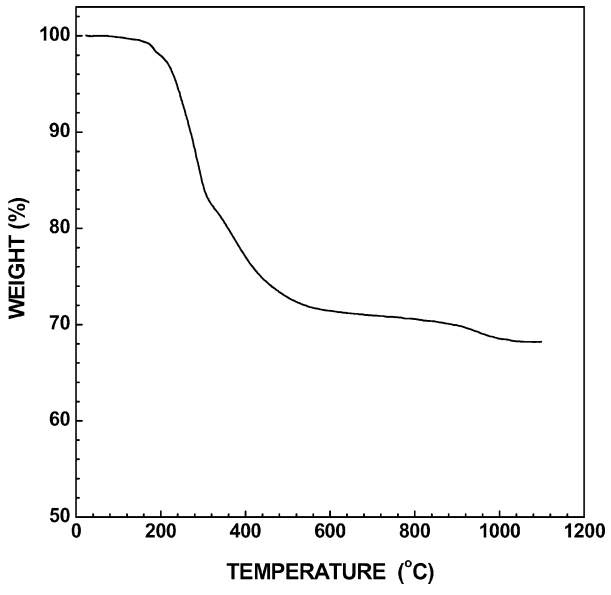

Figure 11 TGA plot of weight loss vs. temperature for an as-dried (120°C) Hf-O-C precursor prepared by solution-based processing.

propoxide/"acacH," 1.4 for HNO_3/Hf, and 16 for H_2O/Hf.) Pyrolytic decomposition of the dried precursor powder was mostly completed (~28 wt% loss) by ~600°C. A gradual weight loss of ~1.5 wt% occurred between 600–900°C and a more rapid weight loss of ~1.5 wt% occurred between 900–1025°C. The decomposition processes were essentially completed by 1050°C; there was no weight loss above this temperature (including during the 1 h hold at 1100°C). The product was a black powder. Heat treatment of this powder in air at 900°C for 1 h produced a white powder with a yield of 84.9%. (X-ray diffraction (XRD) analysis on a separate, but similar, sample showed that the oxidized product was monoclinic hafnium dioxide, *m*-HfO_2.) Thus, the original 1100°C-pyrolyzed product contained 15.1% carbon and a C/HfO_2 molar ratio of 3.1 (i.e., assuming that the pyrolyzed material contained only HfO_2 and C). Hence, the material was slightly carbon-rich compared to the ideal C/Hf molar ratio of 3 for producing stoichiometric HfC by a carbothermal reduction reaction analogous to the one shown in Equation 1 for ZrC.

Fig. 12 shows XRD results for samples heat treated (in argon) in the range of 800–1600°C for 2 h. The weakly crystalline phase in the XRD pattern for the 800°C sample is attributed to tetragonal hafnium oxide (*t*-HfO_2). (The carbon in the sample remained amorphous.) The identification of *t*-HfO_2 is not definitive because it is difficult to distinguish between the tetragonal and orthorhombic phases of HfO_2 [32, 33] as a result of the weak, broad XRD peaks. However, the orthorhombic phase is apparently formed only under high pressure conditions [34, 35], so it seems likely that the HfO_2 in the 800°C sample was the tetragonal phase. Fig. 12 shows that the *t*-HfO_2 became better crystallized after heat treatment at 1100°C. (Once again, it is difficult to rule out definitively the orthorhombic HfO_2 phase because of peak broadening.) The formation of some monoclinic hafnium oxide (*m*-HfO_2) was also observed in the 1100°C sample. In addition, the sample

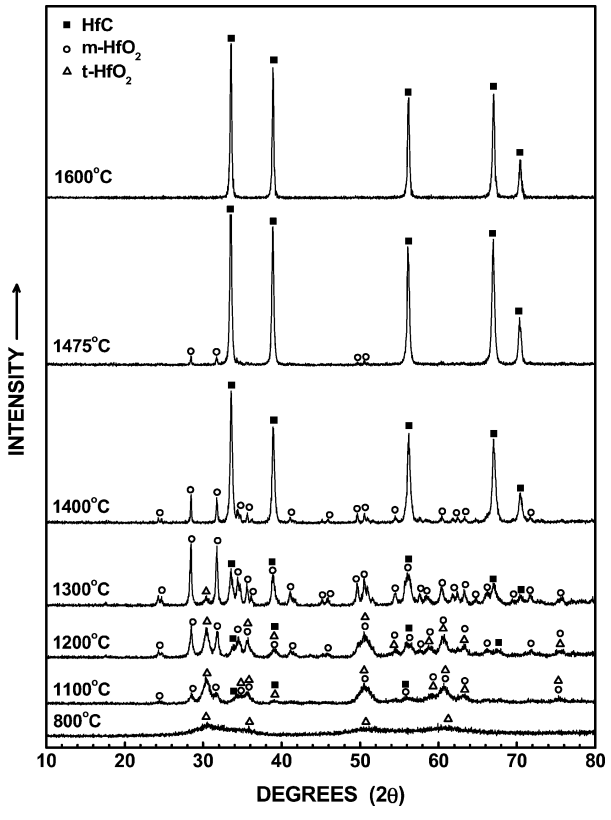

Figure 12 X-ray diffraction (XRD) patterns for heat treated (800–1600°C) samples prepared from a solution-derived Hf-O-C precursor.

appeared to contain a trace of HfC (face-centered cubic) [36]. It is difficult to be certain about the trace presence of HfC because the broad peaks from the HfO_2 phases would overlap with any weak HfC peaks that might be present. However, the XRD pattern for the 1100°C sample shows a very slight shoulder at the 2θ value (~33.4 degrees) for the most intense reflection for HfC (i.e., the (111) peak). Fig. 12 shows that the peak intensities for the HfO_2 phases increased upon further heat treatment at 1200°C, especially for the monoclinic phase. The presence of a small amount of HfC is now clearly evident in the XRD pattern for this sample. The *m*-HfO_2 peak intensities continued to increase significantly in the 1300°C sample, while only a small amount of *t*-HfO_2 phase remained in the sample. The HfC peaks also increased in intensity significantly, although *m*-HfO_2 remained the primary crystalline phase. The phase development observed from 800 to 1300°C in this study can be contrasted to the results reported by Kurokawa *et al*. [18] for samples heat treated in the range of 1000–1300°C. The XRD patterns for all their samples showed a single HfO_2 phase, with relatively broad diffraction peaks, that was very similar to the phase identified as *t*-HfO_2 in Fig. 12. The monoclinic phase was not observed at any heat treatment temperature in their study. In addition, only a trace of HfC was evident in their XRD pattern for a sample heat treated at 1300°C.

Fig. 12 shows that a sample heat treated at 1400°C (2 h) consisted mostly of HfC. The amount of *m*-HfO_2 was reduced substantially compared to the 1300°C sample and no *t*-HfO_2 was present. The HfC peak intensities continued to increase for a sample heat treated at 1475°C and only a trace of *m*-HfO_2 was detected in the

sample. HfC was the only crystalline phase detected in samples heat treated for 2 h at 1600°C (Fig. 12) and at 1800°C (XRD pattern not shown in Fig. 12). Although the 1475°C sample had only a small amount of HfO_2, several experimental observations indicated that the carbothermal reduction reaction still continued to a significant extent at the higher heat treatment temperatures, i.e., just as was observed with the ZrC-based samples. First, there was significant weight loss at heat treatment temperatures above 1475°C. For example, the weight loss upon heat treatment from 1100 to 1475°C was 17.6%, while the weight loss was 23.3% for heat treatment from 1100 to 1800°C. (The latter value is close to the expected weight loss of 22.7% for the ideal HfC carbothermal reduction reaction.) Second, the overall carbon concentration for the 1475°C sample was 8.3 wt%. This value is significantly greater than the value of 6.3 wt% that would be expected if the sample was phase-pure stoichiometric HfC. Hence, it is apparent that the 1475°C sample retained some free carbon (XRD-amorphous) after the heat treatment. Third, a different sample (but with similar overall composition) was heat treated at 1500°C for 2 h and the measured oxygen content was 1.6 wt%. Essentially all of this oxygen must have been dissolved in the HfC lattice because HfO_2 was not observed at all in the XRD pattern for this sample. (This result is consistent with previous studies that have shown that there is considerable solid solubility of HfO_2 in HfC [2, 37]). Fourth, upon heat treatment at 1800°C, the overall carbon concentration decreased from 8.3 wt% for the 1475°C sample to 6.7 wt% for the 1800°C sample. Hence, the continued weight loss above 1475°C can be explained by the same type of carbothermal reduction reaction shown in Equation 2 in which "hafnium oxycarbide," (i.e., HfC with some oxygen dissolved in the lattice) reacts with excess carbon.

Fig. 13 shows plots of the average crystallite sizes (determined by XRD measurements) for each phase (t-HfO_2, m-HfO_2, and HfC) as a function of heat treatment temperature. The t-HfO_2 crystallites that formed initially in the 800°C sample were only ~2.5 nm. The t-HfO_2 crystallite size increased gradually to ~15 nm as the heat treatment temperature increased to 1300°C. The m-HfO_2 crystallites were initially ~17 nm in the 1100°C sample and the size increased rapidly to ~75 nm in the 1400°C sample. This coincides with the period during which most of the carbothermal reduction reaction occurs. The HfC crystallites coarsen more gradually, increasing from ~18 nm in the early stages of the reaction (1200°C sample) to ~34 nm in the 1400°C sample and ~49 nm in the 1475°C sample. (It was not possible to measure an HfC crystallite size for the 1100°C sample because only a trace of HfC was surmised to be present based on a slight shoulder at $2\theta \approx 33.4$ degrees.) The HfC crystallite size increased to an estimated size of ~200 nm in the sample heat treated at 1800°C.

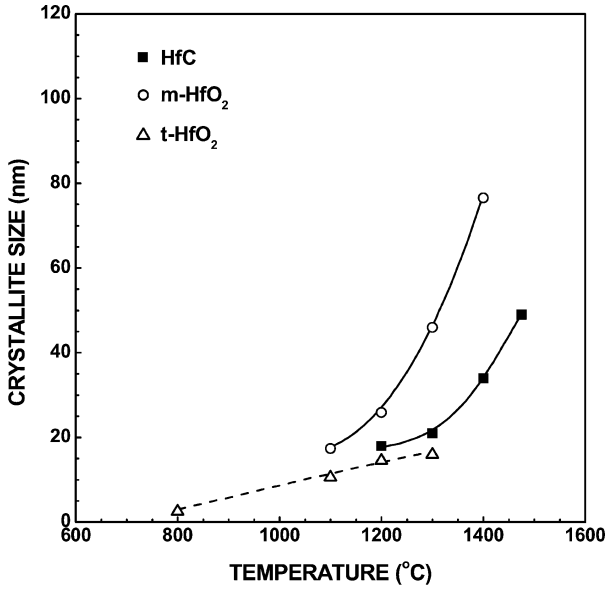

Figure 13 Plot of the t-HfO_2, m-HfO_2, and HfC crystallite sizes (determined from XRD measurements) vs. heat treatment temperature.

The HfC lattice parameter measured for the 1800°C sample was 0.4638 nm which indicates that the composition was near-stoichiometric. (The measured lattice parameter matches the value listed in reference 36. It is also close to values reported for near-stoichiometric HfC by other investigators, although it should be noted that a fairly wide range of values have been reported. [2]) The carbon content measured for the 1800°C sample (6.7 wt%) remained slightly above the value (6.3 wt%) for stoichiometric HfC. However, it was noted earlier that the starting composition (determined for an 1100°C-pyrolyzed sample) was slightly carbon-rich compared to the ideal composition for the reaction analogous to the one shown in Equation 1 for ZrC. Hence, it is reasonable that a small amount of residual carbon would remain in the sample after the carbothermal reduction reaction was completed.

4. Conclusion

Zirconium carbide (ZrC) and hafnium carbide (HfC) powders were produced by carbothermal reduction reactions using fine-scale carbon/metal oxide mixtures as the starting materials. The reactant mixtures were prepared by pyrolytic decomposition of solution-derived precursors. The latter precursors were synthesized via hydrolysis/condensation of metal-organic compounds. The first step in the solution process involved refluxing a metal alkoxide with 2,4 pentanedione ("acacH") in order to partially or fully convert the metal alkoxy groups to a chelated metal diketonate structure ("metal acac"). This was followed by the addition of water (under acidic conditions) in order to promote hydrolysis/condensation reactions. Precursors with variable carbon/metal ratios were produced by varying the concentrations of the solution reactants (i.e., the metal alkoxide, "acacH," water, and acid concentrations). In the Hf-based system, "single-source" precursors could be synthesized which yielded powders with C/HfO_2 molar ratios ≈3.1 after pyrolysis. (This C/HfO_2 ratio was used to produce near-stoichiometric HfC after carbothermal reduction, i.e., according to the Hf-based reaction analogous to Equation 1.) In the Zr-based system, it was necessary to add a secondary soluble carbon source (i.e., phenolic resin or glycerol) during solution

processing in order to obtain a C/ZrO_2 molar ratio ≈3.1 in the pyrolyzed powders.

The phase development during carbothermal reduction was investigated using pyrolyzed powders with carbon/metal oxide molar ratio ≈3.1. The pyrolyzed powders initially consisted of fine-scale mixtures of the tetragonal phase of the metal oxide (ZrO_2 or HfO_2) and amorphous carbon. The tetragonal phase transformed to the monoclinic phase during heat treatment at or above 1100°C. The initial formation of the metal carbide (ZrC or HfC) was clearly evident after heat treatment at 1200°C and the reaction was substantially completed after heat treatments in the range of ~1400–1500°C. HfC and ZrC crystallite sizes (determined by XRD line broadening) were ~50 and ~100–130 nm, respectively, for powders produced at 1475°C. However, weight loss measurements and analyses of the carbon and oxygen contents showed that these samples consisted of metal carbide with some oxygen dissolved in the lattice and some residual free carbon. Heat treatment at higher temperatures (>1600°C) was required to produce near-stoichiometric metal carbides with low oxygen content.

ZrC powders with ~100 nm crystallite size were dry-pressed to form "green" compacts with ~44% relative density. The compacts were sintered at temperatures in the range of 1600–1950°C (2 h). Samples sintered at 1900 and 1950°C had relative densities of ~98 and ~99%, respectively, and zero open porosity.

Acknowledgment

This work was sponsored by the Air Force Office of Scientific Research, USAF, under grant/contract no. F49620-01-1-0112. Experimental contributions by Greg Staab are acknowledged.

References

1. L. E. TOTH, "Transition Metal Carbides and Nitrides" (Academic Press, New York, 1971).
2. A. J. PERRY, *Powder Metall. Int.* **19**(2) (1987) 29.
3. K. UPADHYA, J.-M. YAN and W. P. HOFFMAN, *Bull. Amer. Ceram. Soc.* **76** (1997) 51.
4. R. W. NEWMAN, *Johns Hopkins APL Techn. Dig.* **14**(1) (1993) 24.
5. M. M. OPEKA, I. G. TALMY, E. J. WUCHINA, J. A. ZAYKOSI and S. J. CAUSEY, *J. Eur. Ceram. Soc.* **19** (1999) 2405.
6. F. M. CHARBONNIER, W. A. MACKIE, R. L. HARTMAN and TIANBAO XIE, *J. Vac. Sci. Technol. B* **19** (2001) 1064.
7. B. V. COCKERAM, D. P. MEASURES and A. J. MEULLER, *Thin Solid Films* **355–356** (1999) 17.
8. K. MINATO, T. OGAWA, K. SAWA, A. ISHIKAWA, T. TOMITA, S. IIDA and H. SEKINO, *Nucl. Technol.* **130** (1999) 272.
9. V. I. ZHELANKIN, V. S. KUTSEV and B. F. ORMONT, *Zh. Neorg. Khim.* **3**(5) (1958) 1237.
10. S. K. SARKAR, A. D. MILLER and J. I. MUELLER, *J. Amer. Ceram. Soc.* **55**(1) (1972) 628.
11. C. E. CURTIS, L. M. DONEY and J. R. JOHNSON, *ibid.* **37**(10) (1954) 458.
12. P. G. COTTER and J. A. KOHN, *ibid.* **37**(9) (1954) 415.
13. R. V. SARA, *Trans. AIME* **223** (1965) 1683.
14. E. L. SHAM, E. M. FARFAN-TORRES, S. BRUQUE-GAMEZ and J. J. RODRIGUEZ-JIMENEZ, *Solid State Ion.* **63–65** (1993) 45.
15. H. PREISS, E. SCHIERHORN and K. W. BRZEZINKA, *J. Mater. Sci.* **33** (1998) 4697.
16. I. HASEGAWA, Y. FUKUDA and M. KAJIWARA, *Ceram. Intern.* **25** (1999) 523.
17. Z. HU, M. D. SACKS, G. A. STAAB, C.-A. WANG and A. JAIN, *Ceram. Eng. Sci. Proc.* **23**(4) (2002) 711.
18. Y. KUROKAWA, S. KOBAYASHI, M. SUZUKI, M. SHIMAZAKI and M. TAKAHASHI, *J. Mater. Res.* **13**(3) (1998) 760.
19. B. D. CULLITY, "Elements of X-ray Diffraction" (Addison-Wesley Publishing Co., Reading, MA, 1967).
20. D. C. BRADLEY, R. C. MEHROHTRA and W. WARDLAW, *J. Chem. Soc. (London)* (1953) 1634.
21. C. D. GAGLIARDI and K. A. BERGLUND, in "Processing Science of Advanced Ceramics", edited by I. A. Aksay, G. L. McVay and D. R. Ulrich (Mat. Res. Soc. Symp. Proc., Mater. Res. Soc., Pittsburgh, PA, 1989) Vol. 155, p. 127.
22. K. CONSTANT, R. KIEFFER and P. ETTMAYER, *Monatshefte fur Chemie* **106** (1975) 823.
23. A. OUENSANGA, A. PIALOUX and M. DODE, *Rev. Int. Hautes Temp. Refract.* **11** (1974) 289.
24. A. MAITRE and P. LEFORT, *Solid State Ionics* **104** (1997) 109.
25. V. P. BULYCHEV, R. A. ANDRIEVSKII and L. B. NEZHEVENKO, *Poroshkovaya Metallurgia* **172**(4) (1977) 38.
26. L. B. NEZHEVENKO, I. I. SPIVAK, P. V. GERASIMOV, B. D. GUREVICH and V. N. RYSTSOV, *ibid.* **212**(8) (1980) 23.
27. A. G. LANIN, E. V. MARCHEV and S. A. PRITCHIN, *Ceram. Intern.* **17** (1991) 310.
28. P. BARNIER, C. BRODHAD and F. THEVENOT, *J. Mater. Sci.* **21** (1986) 2547.
29. C. T. LYNCH, K. S. MAZDIYASNI, J. S. SMITH and W. J. CRAWFORD, *Anal. Chem.* **36**(12) (1964) 2332.
30. R. C. FAY and T. J. PINNAVAIA, *Inorg. Chem.* **7**(3) (1968) 508.
31. B. ALLARD, *J. Inorg. Nucl. Chem.* **38** (1976) 2109.
32. Powder Diffraction File Card No. 08-0342 (tetragonal hafnium oxide, HfO_2), JCPDS—International Centre for Diffraction Data, Newtown Square, PA.
33. Powder Diffraction File Card No. 21-0904 (orthorhombic hafnium oxide, HfO_2), JCPDS—International Centre for Diffraction Data, Newtown Square, PA.
34. G. BOCQUILLON, C. SUSSE and B. VODAR, *Rev. Int. Hautes Temp. Refract.* **5** (1968) 247.
35. O. OHTAKA, T. YAMANAK and S. KUME, *J. Ceram. Soc. Jpn.* **99** (1991) 826.
36. Powder Diffraction File Card No. 39-1491 (cubic hafnium carbide, HfC), JCPDS—International Centre for Diffraction Data, Newtown Square, PA.
37. K. CONSTANT, R. KIEFFER and P. ETTMAYER, *Monatshefte fur Chemie* **106** (1975) 973.

Received 22 October 2003
and accepted 23 February 2004